SAND2022-16382C

System Integration for Grid-scale Hybrid Battery Technologies

Oindrilla Dutta, Jacob Mueller, Robert Wauneka, and Valerio De Angelis, *Members, IEEE*
Sandia National Laboratories, Albuquerque, NM 87185
email: odutta@sandia.gov, jmuelle@sandia.gov, rwaunek@sandia.gov, and vdeange@sandia.gov

***Abstract*—In this work, a modular and open-source platform has been developed for integrating hybrid battery energy storage systems that are intended for grid applications. Alongside integration, this platform will facilitate testing and optimal operation of hybrid storage technologies. Here, a hardware testbed and a control software have been designed, where the former comprises commercial Lithium-iron-phosphate ($LiFePO_4$) and Lead Acid ($Pb-acid$) cells, custom built Dual Active Bridge (DAB) DC-DC converters, and a commercial DC-AC conversion system. In this testbed the batteries have an operating voltage range of $\backsim$11-15V, the DC-AC conversion stage has a DC link voltage of 24V, and it connects to a 208V 3-ϕ grid. The hardware testbed can be scaled up to higher voltages. The control software is developed in Python, and the firmware for all the hardware components is developed in C. This software implements hybrid charge/discharge protocols that are suitable for each battery technology for preventing cell degradation, and perform uninterrupted quality checks on selected battery packs. The developed platform provides flexibility, modularity, safety and economic benefits to utility-scale storage integration.**

***Index Terms*—Batteries, Energy management system, Dual Active Bridge, Hybrid energy storage, Lead-Acid, Lithium-iron-phosphate.**

I. Introduction

BATTERY Energy Storage Systems (BESSs) have become essential for utility grids that are characterized by high penetration of renewable resources. Grid services supported by batteries vary widely in their requirement for power rating, energy capacity, ramp rate, annual cycling, and hours of operation [1]. For instance, congestion relief requires 1-4 hours of discharge with 100 cycles/annum, whereas voltage regulation needs half an hour support without any cycling, and frequency stabilization requires a response time in seconds-minutes [2]. Thus, technologies beyond Li-ion will be essential for optimal performance in the various aspects of generation, transmission and distribution [3], [4]. Besides, it will become necessary to combine batteries with disparate state of health, such as old and new cells [5]. Hence, combining hybrid battery technologies will be necessary for long duration energy storage.

A BESS is a complex structure comprising multiple components. The core component is a cell, such as Pb-acid or Ni-metal-hydride cells, which account for nearly 30% of the total cost and these technologies are still relatively new. Hence, system integration using hybrid batteries is technically complex and requires coordination among the controllers of the various system constituents [6], [7]. Presently, there is no standardization of the power electronic topology, communication protocol, and control software for integrating and operating grid-scale batteries. This has often led to accidents during which thermal runaway from a single cell quickly propagates through an entire rack, thereby destroying an entire installation [8].

Topologies for integrating batteries to the grid can be categorized by how they interface with the DC-AC conversion stage [9]. In an uncontrolled or passive configuration, storage modules are directly connected to an inverter's DC link [10]. In semi-controlled or semi-active configurations, a subset of storage modules connect directly to an inverter's DC link, while others are interfaced through dedicated DC-DC converters for individualized control [11]. In fully-controlled or active configurations, all storage modules are interfaced through dedicated DC-DC converters, which typically connect in parallel at the inverter's DC link [12], [13].

The Passive topology is commonly adopted by utilities for its simplicity [9]. This topology is, however, ineffective for combining hybrid batteries as different technologies have distinct charge/discharge protocols and operate within different voltage ranges [14]. These operating voltage ranges change as the cells age [15]. Other drawbacks of this topology include the inability of mixing batteries with disparate states of health, continuous connection of the battery modules to a DC-AC converter, compatibility of the DC-AC system with the integrating battery technology, alongside active and passive balancing for increasing operational window.

Active configurations enable independent control over individual battery module behavior, which can be leveraged for critical improvements to the reliability and operational flexibility of utility-scale energy storage. In particular, full controllability may enable reductions in battery degradation through improved charge/discharge current quality [16], implementation of hybrid and adaptive cycling protocols, active mitigation of propagating thermal runaway events, improved state of health monitoring [17], and "hot swap" replacement of aged batteries. Existing literature on hybrid storage for utility applications using active topology focuses on stabilizing DC-link voltage and optimizing grid performance [18], [19]. These studies lack any demonstration of hybrid cycling of mixed battery chemistries. There is also a dearth of discussion on control strategies and converter topologies for improving battery state of health. Besides, the control software is ad-hoc, and not designed to perform with different system configurations.

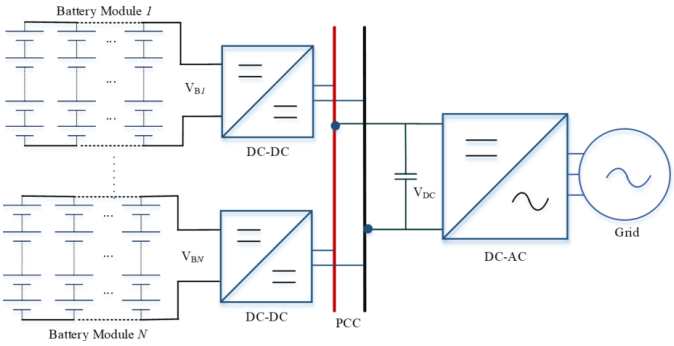

Fig. 1. Active connection topology for integrating hybrid battery modules.

In this work, we have developed a modular and open-source hardware platform and a control software for grid integration of BESSs using the active connection topology, as shown in Fig. 1. The hardware and software platform are designed to exhibit following key advantages:

- Flexibility: Different battery technologies are characterised by a widely varying operating voltage range, which changes as the battery cells age. Also, the battery cycling protocol varies among the different chemistries, as shown in Table I. Active connection topology provides the flexibility of operating different battery technologies with their suitable charge/discharge protocol.
- Modularity: In active topology, battery modules are not required to be continuously connected to a DC-AC converter's DC-link in order to bring it online. Also, damaged cells can be replaced without shutting down the entire energy storage installation. This topology also facilitates mixing batteries of disparate state of health.
- Safety: Thermal runaway in a single battery cell can rapidly propagate to the adjacent cells, thereby causing catastrophic accidents that destroy an entire installation. In active connection, the DC-DC converters can isolate a stationary fire by disconnecting the affected cells prior to the propagation of fire.
- Economic justification: Addition of a DC-DC converter increases installation cost. The lifetime of power electronics and solar panels is 10-20 years. Over the lifetime of an installation, batteries will be completely or partially replaced at least twice. This fact, along with safety, reduced cell ageing and the ease of recycling old batteries, provide the necessary stack benefit for economic justification. Besides, standardization of energy storage system integration process and control software will further reduce the installation cost.

TABLE I
CHARGING PROTOCOL OF BATTERY TECHNOLOGIES

Battery Type	Charge Protocol
Lithium-ion	CC-CV-Rest
Lead-acid	CC-CV-Rest-Float
Zn-Based ($Ni-Zn$, MnO_2-Zn...)	CC-Rest-CC-Rest

CC-Constant Current CV-Constant Voltage

II. PLATFORM DEVELOPMENT

This section provides a detailed description of the developed platform, comprising a hardware testbed and a control flowchart, as depicted by the schematic in Fig. 2.

A. Hardware Testbed

The hardware testbed comprises two parallel strings of battery packs, where string-A is a pack of four commercial $LiFePO_4$ cells connected in series, and string-B is a pack of six commercial $Pb-acid$ cells that are also connected in series (Fig. 2). Each battery string is interfaced with a DAB DC-DC converter. The two DAB converters connect in parallel at a point of common coupling (PCC). This PCC is interfaced with a Regenerative Power Supply (RPS) which emulates the behavior of an inverter's DC link. The RPS synchronizes with 208V 3-ϕ grid. A hardware testbed, as shown in Fig. 3, has been built to UL 1973 specifications based on the system schematic in Fig. 2. This hardware testbed is modular and plug-play. Each constituent of this testbed is described in the subsequent sections.

1) Battery Technologies: Some applications and manufacturer specifications of the two types of battery technologies, $LiFePO_4$ and $Pb-acid$, are tabulated in Table II. As illustrated in Fig. 3, each battery string is enclosed in a 3D printed box that is made of Ultem 1010, which is a fire-proof material. Fig. 3 also shows that each battery pack is connected to an Orion battery management system (BMS). The Orion-BMS is used to obtain measurements of the string current and cell voltages in each battery module.

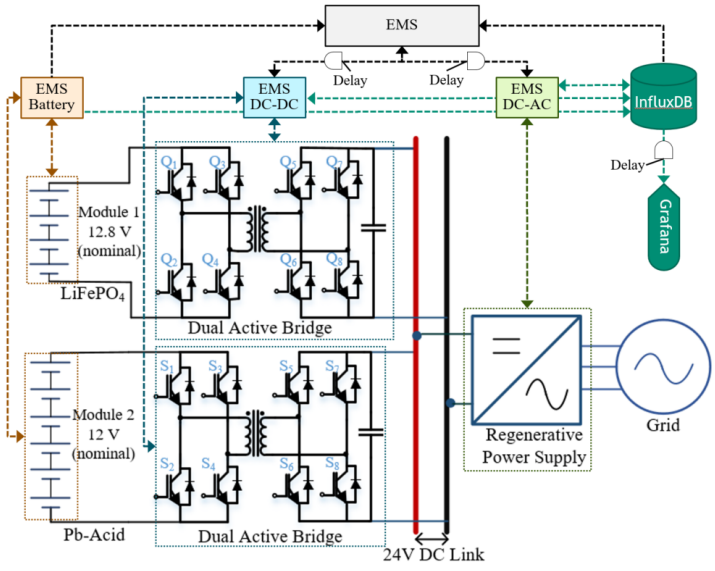

Fig. 2. Schematic of the developed hardware and control software platform.

Fig. 3. Hardware setup developed for testing hybrid battery system that consists of Lithium-iron-phosphate and Lead-acid battery packs.

TABLE II
SPECIFICATIONS OF BATTERY TECHNOLOGIES

Parameter	LiFePO4	Pb-Acid
Manufacturer	Power Sonic	Enersys Cyclon
Nominal voltage	3.2 V	2 V
Rated capacity	25 Ah	25 Ah
Recommended charging	1C CC charge to 3.65V then CV until current <0.05C	CV charging: Fast chargers 2.45 to 2.5V, Float chargers 2.27 to 2.35 V

2) DC-DC Converter: This section provides a brief overview of the DAB DC-DC topology. The DAB converter is developed at the Advanced Power Electronic Conversion System laboratory (APEX) of Sandia National Labs (SNL), which is described in our previous work [6]. A schematic of the DAB topology and a snapshot of the hardware prototype are illustrated in Fig. 4.

The DAB circuit topology has been chosen for this application due to its galvanic isolation, high switching frequency with soft switching, and high power density [20]. Power transfer between the two bridges in a DAB is guided by the phase difference (ψ) between the primary (V_p) and secondary (V_s) voltages, as represented by (1).

$$P_{DAB} = \frac{nV_pV_s\psi(\pi-\psi)}{2\pi^2 f_{sw}L_{leak}} \tag{1}$$

where ψ is a function of the battery voltage (V_B), switching frequency (f_{sw}), leakage inductance (L_{lrak}), output voltage

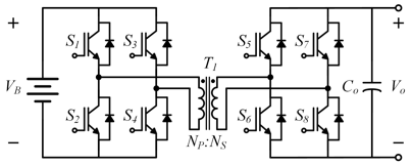

(a) Circuit schematic.

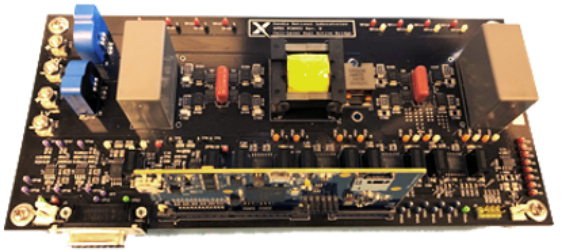

(b) Hardware prototype designed and built at Sandia National Labs.

Fig. 4. Dual Active Bridge (DAB) DC-DC Converter.

(V_o), output power (P_{out}), and turns ratio (n), as shown in (2).

$$\psi = \frac{\pi}{2}\left[1-\sqrt{1-8\frac{f_{sw}L_{leak}P_{out}}{nV_BV_o}}\right] \tag{2}$$

In this work, the DAB parameters have been designed for a nominal power of 75W with nominal V_B and V_o of 12 and 24V, respectively. This DAB provides $\simeq 95\%$ efficiency and can be operated in both current control and voltage control operating modes. Fig. 5 shows the DAB control loop, where a proportional-integral (PI) controller is used to regulate the phase shift (ψ) based on the difference between the measured

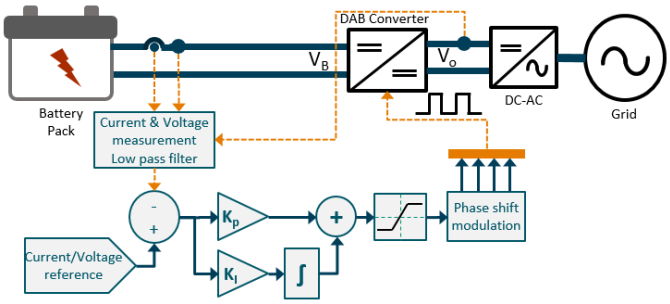

Fig. 5. Dual Active Bridge control loop based on phase shift modulation.

and the reference values for voltage/current. The phase shift modulation block provides switching signals at 100 kHz switching frequency to the eight switches in the DAB. This control loop has been implemented in a Texas Instrument C2000 ControlCard.

3) DC-AC Conversion: An RPS of Keysight's RPS793xA series is interfaced to the PCC DC bus, as shown in Fig. 3. On the AC side, he RPS is connected to a Grid Emulator, which provides $3-\phi$ 208V, 60Hz. The RPS is responsible for maintaining the PCC voltage at 24V during both charging and discharging operation of the two battery packs. It also performs as a load, thereby acting as a bidirectional power source.

B. Control Software and Firmware

This section describes the process of developing an open-source and modular software/firmware platform that is shown in Fig. 6.

The outermost layer in the software is the Energy Management System (EMS), which is developed in Python. This EMS controls and coordinates the operation of the different constituents of an ESS, based on a user-defined configuration file. This configuration file contains information about the system, such as, the number of battery modules, the type

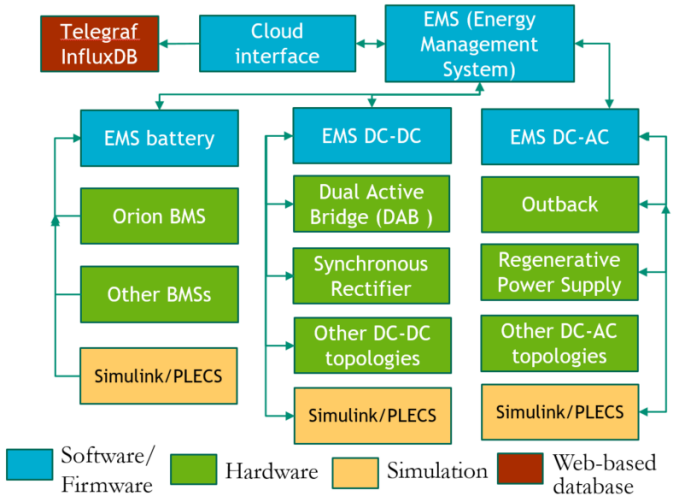

Fig. 6. Open source and modular control software and firmware.

of battery cells, the DC-DC and DC-AC converter topologies, the type of communication protocol, and manufacturer specifications of the different devices. Figs. 2 and 6 describe how the EMS generates individual control threads for each system constituent, such as, the EMS battery for the battery modules, the EMS DC-DC for the two DAB converters, and the EMS DC-AC for the RPS in this particular system setup. These individual control threads are all executed in parallel. The EMS also initiates a remote data acquisition (DAQ) and monitoring system, which is open-sources, open-access, and can be used to consolidate data from different projects. The data is gathered in InfluxDB and visualized in Grafana. The data acquisition is executed in parallel with the other control threads. Delays are introduced in these parallel threads for coordinating their operation and preventing any sample aliasing.

The EMS software can be used to operate a system in both simulation and hardware environment. Firmware for different types of devices/equipments/simulation-environments have been developed and included in a repository in this software platform. New firmware can be added to this repository for future development.

Fig. 7 shows the control flowchart for the system schematic described in Fig. 2. The firmware layer is directly associated with the Orion-BMS registers, the Texas Instrument ControlCard, and the RPS through serial communication. Firmware for the Texas Instrument ControlCard is programmed in C, whereas the same for the RPS is programmed using SCPI commands. The EMS block interacts with the firmware layers for the battery packs, the DABs and the RPS through the EMS Battery, EMS DC-DC, and EMS DC-AC blocks, respectively. The sequence of control steps executed by the EMS block for cycling battery packs is as follows:

- The EMS block first acquires system information, which is specified in a user-defined configuration file, through the EMS System block.
- Based on the system information, the EMS block initializes the EMS Battery, EMS DC-DC, and the EMS DC-AC blocks.
- The EMS block then initiates the DAQ block, which is responsible for acquiring measurements from the EMS Battery, EMS DC-DC, and the EMS DC-AC blocks. This DAQ block then uploads the data to InfluxDB, which is a web-based database. This database facilitates data visualization from remote access points.
- The EMS DC-DC and DAQ blocks are executed as parallel threads along with an emergency STOP operation. This STOP operation is a graphical user interface that is designed to interrupt program execution based on user input.
- The EMS block then sets the RPS voltage to 24V through the EMS DC-AC block.
- Starting the RPS creates voltage transients at the high voltage side of the DABs, which halts the DABs. Hence, the EMS block resets the DABs by sending a reset command to the EMS DC-DC block.

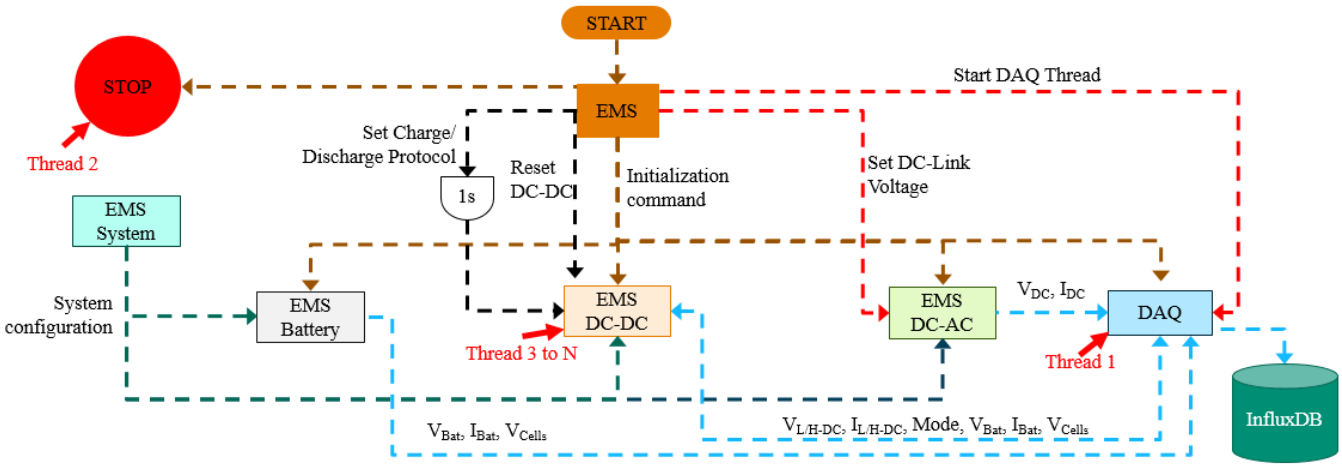

Fig. 7. Energy management system control flowchart.

- The EMS block then sends charge or discharge commands to the EMS DC-DC block. These charge/discharge commands are based on the protocols that are suitable for the battery technologies that are interfaced with each DC-DC converter.

III. Case Studies

This section describes two case studies for hybrid charging and discharging of the $LiFePO_4$ and $Pb-Acid$ battery modules.

A. Case Study I: Hybrid Charging

In this case study the four $LiFePO_4$ cells are charged at 5A constant current (CC) until the highest cell voltage reaches 3.6V, after which the cells are rested. The six $Pb-Acid$ cells are charged at 5A CC until the highest cell voltage reaches 2.3V, after which the control is shifted to constant voltage (CV). CV charging is continued until the highest cell voltage reaches 2.35V, after which cells are relaxed.

Figs. 8a and 8b show the results corresponding to this case study, as observed in the web-based interface. These figures show that a transition from CC to CV in the $Pb-acid$ battery pack does not impact the $LiFePO_4$ battery pack. Data in the web-based interface is obtained at an interval of 19s. Any system transient cannot be observed at such slow sampling interval. Hence, the oscilloscope data during the transition form CC to CV is illustrated in Figs. 9a and 9b, which ascertain the decoupling of operation in the two different battery technologies. Voltage and current ripples in the two battery modules at the DAB switching frequency of 100 kHz are illustrated in Figs. 10a and 10b, which show the batteries are charged with good quality current.

The cell voltages corresponding to this case study are shown in Figs. 11a and 11b. These illustrations show significant cell to cell variation in cell-4 of the $Pb-acid$ pack. It is crucial to observe cell to cell imbalance since this causes accelerated degradation of battery modules.

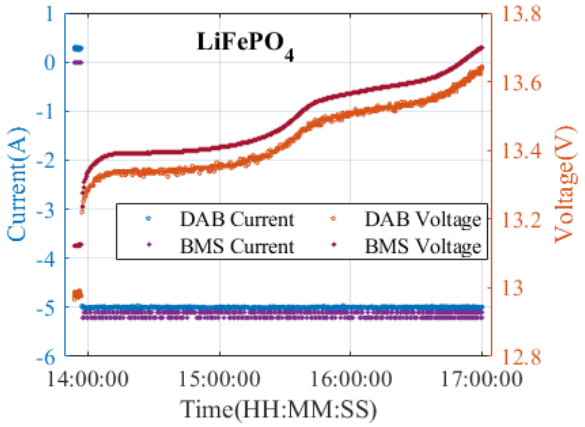

(a) Voltage and current of the $LiFePO_4$ string as monitored by the web-based interface. These measurements are based on the data from the Orion-BMS and the sensors on the DAB board.

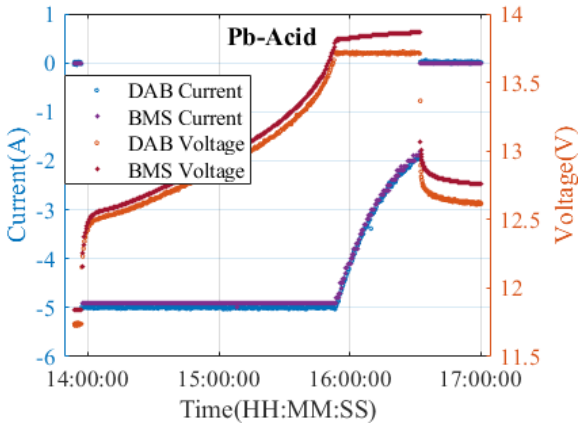

(b) Voltage and current of the $Pb-Acid$ string as monitored by the web-based interface. These measurements are based on the data from the Orion-BMS and the sensors on the DAB board.

Fig. 8. Voltage and current measurements for CC charging of $LiFePO_4$ battery pack and CC-CV charging of $Pb-Acid$ battery pack.

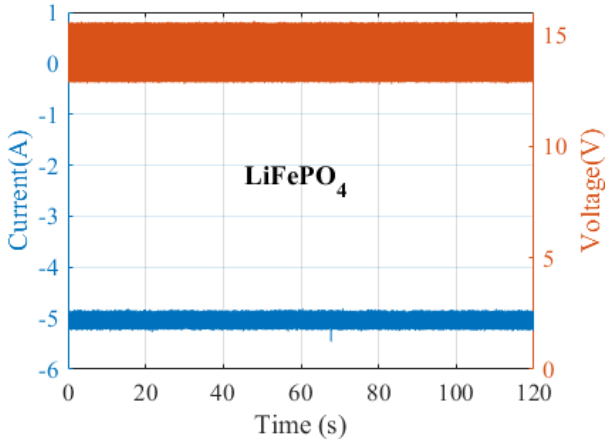

(a) Voltage and current of the $LiFePO_4$ string as monitored by the oscilloscope.

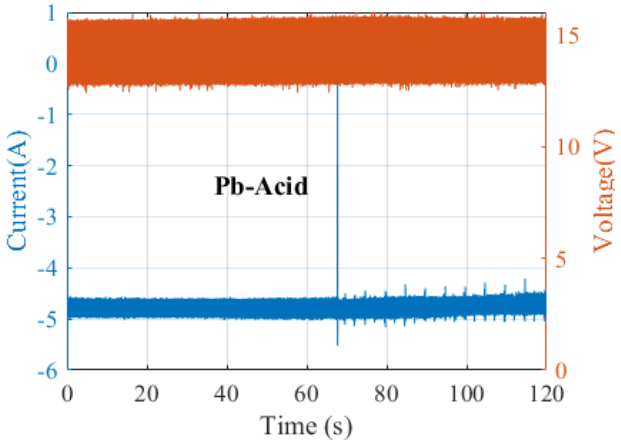

(b) Voltage and current of the $Pb-Acid$ string as monitored by the oscilloscope.

Fig. 9. Voltage and current measurements for CC charging of $LiFePO_4$ battery pack and CC-CV charging of $Pb-Acid$ battery pack as monitored by the oscilloscope.

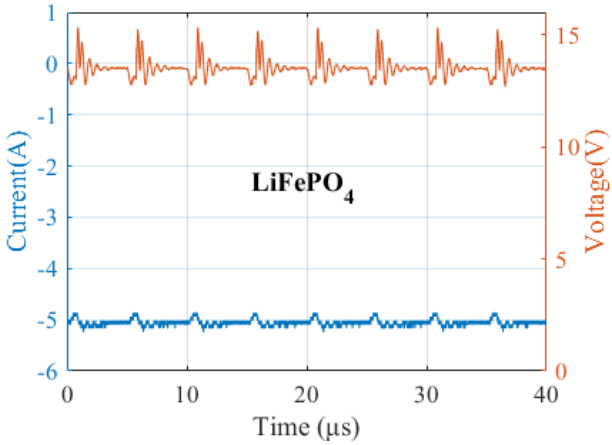

(a) Voltage and current of the $LiFePO_4$ string as monitored by the oscilloscope.

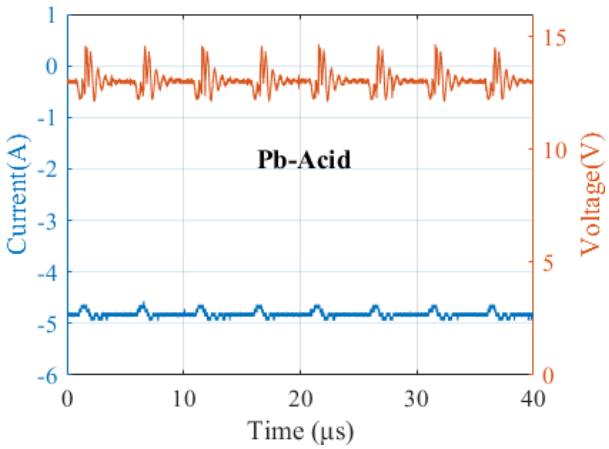

(b) Voltage and current of the $Pb-Acid$ string as monitored by the oscilloscope.

Fig. 10. Voltage and current measurements for CC charging of $LiFePO_4$ battery pack and CC-CV charging of $Pb-Acid$ battery pack as monitored by the oscilloscope.

B. Case Study II: Pulse Discharging

Pulse tests on battery cells are necessary for estimation of battery parameters. In commercially existing connection topologies, in-situ parameter estimation cannot be performed without disrupting the entire operation. In this case study pulse discharging has been performed on the $Pb-Acid$ battery pack for estimating its parameters. This pulse test is performed while the $LiFePO_4$ battery pack continues to discharge at 5A. Figs. 12 and 13 show the cell voltages and string currents, respectively, during the pulse discharge test on the $Pb-Acid$ battery pack.

IV. Conclusion and Future Work

This work shows the development and validation of a modular open-source platform for testing and operating any commercial battery technology using custom built DC-DC and commercial DC-AC converters.

A modular hardware testbed has been built, which can accommodate different types of batteries, battery management systems, DC-DC converters, protection devices and communication methods. A Python based open-source and modular control software/firmware has been developed, which is capable of interfacing with different system configurations in both hardware and software environment. This software uploads real-time system measurements to a public web-based interface to remotely monitor and consolidate data from multiple systems for further analysis. Firmware libraries have also been developed for the different system constituents.

The developed platform has demonstrated hybrid charging of $LiFePO_4$ and $Pb-Acid$ battery modules at different voltage levels, and pulse discharging of the $Pb-Acid$ battery module. The hardware results show reduced ripple in battery cycling current and stable performance with hybrid cycling of the two different battery technologies.

Going forward, this platform will be tested with different

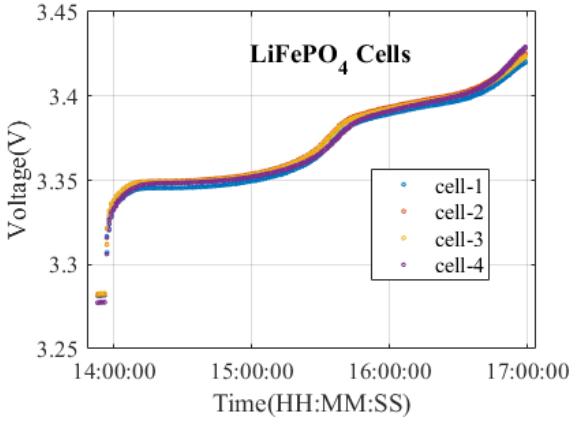

(a) Voltages of the four $LiFePO_4$ cells as monitored by the web-based interface.

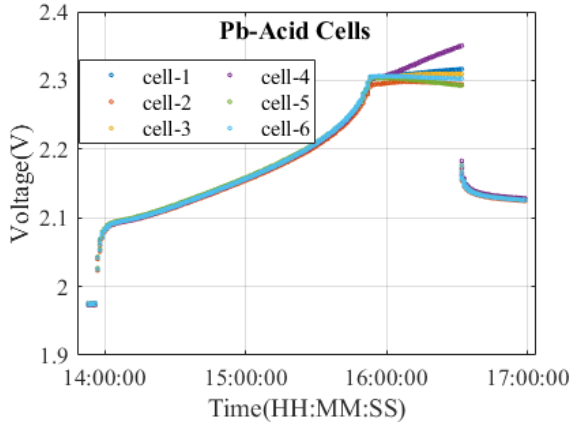

(b) Voltages of the six $Pb-Acid$ cells as monitored by the web-based interface.

Fig. 11. Cell voltages for CC charging of $LiFePO_4$ battery pack and CC-CV charging of $Pb-Acid$ battery pack as monitored by the oscilloscope.

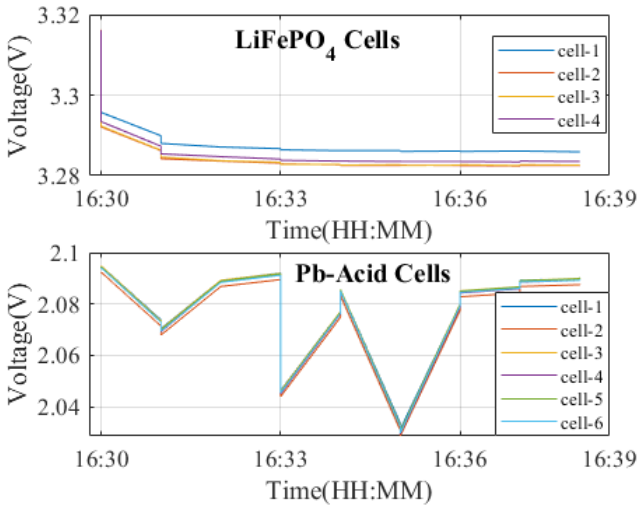

Fig. 12. Cell voltages of the $LiFePO_4$ and $Pb-Acid$ battery technologies during CC discharge of the $LiFePO_4$ pack at 5A and pulse discharge of the $Pb-Acid$ pack.

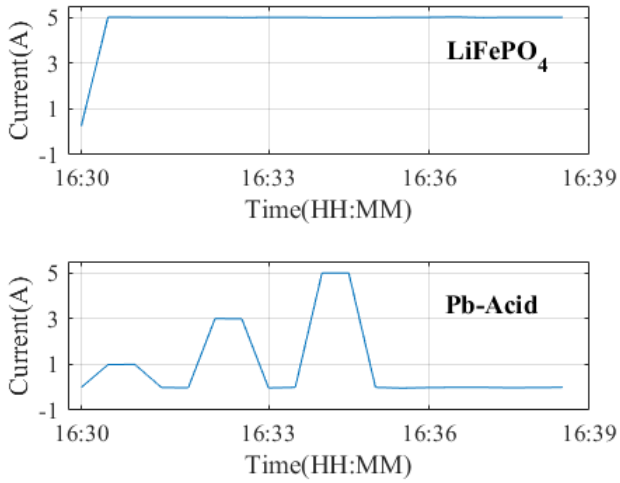

Fig. 13. String currents of the $LiFePO_4$ and $Pb-Acid$ battery technologies during CC discharge of the $LiFePO_4$ pack at 5A and pulse discharge of the $Pb-Acid$ pack.

load profiles and faster communication protocols for improvising the control software. A low-cost DC-AC converter hardware will be designed with a high DC/AC Voltage ratio and a control strategy that is suitable for integrating BESSs to the grid. Additional sensors will be provided to the BMS for advanced safety. The authors will make this platform available to universities as a research platform and companies as a robust system to deploy new battery technologies in the field.

ACKNOWLEDGMENT

We would like to thank Dr. Imre Gyuk, Director of Energy Storage Research, for his support. Sandia National Laboratories is a multi-mission laboratory managed and operated by National Technology and Engineering Solutions of Sandia, LLC., a wholly owned subsidiary of Honeywell International, Inc., for the U.S. Department of Energy National Nuclear Security Administration under contract DE-NA-0003525.

REFERENCES

[1] M. T. Lawder, B. Suthar, P. W. Northrop, S. De, C. M. Hoff, O. Leitermann, M. L. Crow, S. Santhanagopalan, and V. R. Subramanian, "Battery energy storage system (bess) and battery management system (bms) for grid-scale applications," *Proceedings of the IEEE*, vol. 102, no. 6, pp. 1014–1030, 2014.

[2] T. S. Babu, K. R. Vasudevan, V. K. Ramachandaramurthy, S. B. Sani, S. Chemud, and R. M. Lajim, "A comprehensive review of hybrid energy storage systems: Converter topologies, control strategies and future prospects," *IEEE Access*, vol. 8, pp. 148 702–148 721, 2020.

[3] S. Vazquez, S. M. Lukic, E. Galvan, L. G. Franquelo, and J. M. Carrasco, "Energy storage systems for transport and grid applications," *IEEE Transactions on industrial electronics*, vol. 57, no. 12, pp. 3881–3895, 2010.

[4] B. B. McKeon, J. Furukawa, and S. Fenstermacher, "Advanced lead–acid batteries and the development of grid-scale energy storage systems," *Proceedings of the IEEE*, vol. 102, no. 6, pp. 951–963, 2014.

[5] M. T. Smith, M. R. Starke, M. Chinthavali, and L. M. Tolbert, "Architecture for utility-scale multi-chemistry battery energy storage," in *2019*

IEEE Energy Conversion Congress and Exposition (ECCE), 2019, pp. 5386–5392.

[6] O. Dutta, J. Mueller, R. Wauneka, V. De Angelis, and D. Rosewater, "Integrated power converters for optimal operation of hybrid battery packs," in *2022 IEEE Power & Energy Society General Meeting (PESGM)*. IEEE, 2022, pp. 1–5.

[7] B. R. Ravada, N. R. Tummuru, and B. N. L. Ande, "A grid-connected converter configuration for the synergy of battery-supercapacitor hybrid storage and renewable energy resources," *IEEE Journal of Emerging and Selected Topics in Industrial Electronics*, vol. 2, no. 3, pp. 334–342, 2021.

[8] "Bess failure event database," Available at https://storagewiki.epri.com/index.php/BESS_Failure_Event_Database.

[9] G. Wang, G. Konstantinou, C. D. Townsend, J. Pou, S. Vazquez, G. D. Demetriades, and V. G. Agelidis, "A review of power electronics for grid connection of utility-scale battery energy storage systems," *IEEE Transactions on Sustainable Energy*, vol. 7, no. 4, pp. 1778–1790, 2016.

[10] X. Li and S. Wang, "Energy management and operational control methods for grid battery energy storage systems," *CSEE Journal of Power and Energy Systems*, vol. 7, no. 5, pp. 1026–1040, 2019.

[11] R. Shi, S. Semsar, and P. W. Lehn, "Single-stage hybrid energy storage integration in electric vehicles using vector controlled power sharing," *IEEE Transactions on Industrial Electronics*, vol. 68, no. 11, pp. 10 623–10 633, 2020.

[12] S. K. Kollimalla, M. K. Mishra, A. Ukil, and H. B. Gooi, "Dc grid voltage regulation using new hess control strategy," *IEEE Transactions on Sustainable Energy*, vol. 8, no. 2, pp. 772–781, 2017.

[13] O. Dutta, M. Saleh, M. Khodaparastan, and A. Mohamed, "A dual-stage modeling and optimization framework for wayside energy storage in electric rail transit systems," *Energies*, vol. 13, no. 7, p. 1614, 2020.

[14] V. De Angelis and Y. Preger, "Batteryarchive. org? insights from a public repository for visualization analysis and comparison of battery data across institutions." Sandia National Lab.(SNL-NM), Albuquerque, NM (United States), Tech. Rep., 2021.

[15] Z. Deng, X. Hu, X. Lin, L. Xu, Y. Che, and L. Hu, "General discharge voltage information enabled health evaluation for lithium-ion batteries," *IEEE/ASME Transactions on Mechatronics*, vol. 26, no. 3, pp. 1295–1306, 2021.

[16] F. Chang, F. Roemer, and M. Lienkamp, "Influence of current ripples in cascaded multilevel topologies on the aging of lithium batteries," *IEEE Transactions on Power Electronics*, vol. 35, no. 11, pp. 11 879–11 890, 2020.

[17] S. B. Vilsen and D.-I. Stroe, "Transfer learning for adapting battery state-of-health estimation from laboratory to field operation," *IEEE Access*, vol. 10, pp. 26 514–26 528, 2022.

[18] J. Xiao, P. Wang, and L. Setyawan, "Multilevel energy management system for hybridization of energy storages in dc microgrids," *IEEE Transactions on Smart Grid*, vol. 7, no. 2, pp. 847–856, 2015.

[19] U. Manandhar, N. R. Tummuru, S. K. Kollimalla, A. Ukil, G. H. Beng, and K. Chaudhari, "Validation of faster joint control strategy for battery- and supercapacitor-based energy storage system," *IEEE Transactions on Industrial Electronics*, vol. 65, no. 4, pp. 3286–3295, 2018.

[20] J. A. Mueller and J. W. Kimball, "Modeling dual active bridge converters in dc distribution systems," *IEEE Transactions on Power Electronics*, vol. 34, no. 6, pp. 5867–5879, 2018.